nature chemical biology

ARTICLE

PUBLISHED ONLINE: 28 FEBRUARY 2017 | DOI: 10.1038/NCHEMBIO.2320

The *Arabidopsis O*-fucosyltransferase SPINDLY activates nuclear growth repressor DELLA

Rodolfo Zentella[1,7], Ning Sui[1,7], Benjamin Barnhill[2], Wen-Ping Hsieh[1], Jianhong Hu[1], Jeffrey Shabanowitz[2], Michael Boyce[3], Neil E Olszewski[4], Pei Zhou[3,5], Donald F Hunt[2,6] & Tai-ping Sun[1]*

Plant development requires coordination among complex signaling networks to enhance the plant's adaptation to changing environments. DELLAs, transcription regulators originally identified as repressors of phytohormone gibberellin signaling, play a central role in integrating multiple signaling activities via direct protein interactions with key transcription factors. Here, we found that DELLA is mono-O-fucosylated by the novel *O*-fucosyltransferase SPINDLY (SPY) in *Arabidopsis thaliana*. O-fucosylation activates DELLA by promoting its interaction with key regulators in brassinosteroid- and light-signaling pathways, including BRASSINAZOLE-RESISTANT1 (BZR1), PHYTOCHROME-INTERACTING-FACTOR3 (PIF3) and PIF4. Moreover, *spy* mutants displayed elevated responses to gibberellin and brassinosteroid, and increased expression of common target genes of DELLAs, BZR1 and PIFs. Our study revealed that SPY-dependent protein O-fucosylation plays a key role in regulating plant development. This finding may have broader importance because SPY orthologs are conserved in prokaryotes and eukaryotes, thus suggesting that intracellular O-fucosylation may regulate a wide range of biological processes in diverse organisms.

Plant adaptation and survival require strict coordination of internal signaling pathways in response to external biotic and abiotic cues[1]. The DELLA proteins are a class of important central integrators of multiple signaling pathways in flowering plants. DELLAs were initially identified as repressors of the phytohormone gibberellin (GA) signaling[2,3]. Recent studies have further revealed that DELLAs are master growth repressors[4,5] that restrict plant growth by causing transcriptional reprogramming of genes functioning in cell division, expansion and differentiation, through direct protein-protein interactions with key transcription factors[6–8]. DELLAs contain a conserved N-terminal DELLA domain, which is required for degradation induced by the GA-receptor GID1 complex[9–12], followed by a divergent and disordered sequence rich in serine and threonine residues (poly(S/T)) and a conserved C-terminal GRAS domain with transcription-regulator function[2,8,13] (**Fig. 1a**). Internal deletions of the DELLA motif (for example, *gai-1* and *rga-Δ17* in *Arabidopsis*) result in a constitutively active repressor that does not respond to GA-induced degradation[3,14]. The dwarf phenotype of these dominant DELLA mutants is partially rescued by hypomorphic *spy* alleles[15,16]. Both SPY and its paralog SECRET AGENT (SEC) in *Arabidopsis* are predicted to encode O-linked β-*N*-acetylglucosamine (*O*-GlcNAc) transferases (OGTs), each of which contains an N-terminal protein-interaction domain (tetratricopeptide repeats (TPRs)) and a C-terminal putative OGT catalytic domain[17–19] (**Supplementary Results** and **Supplementary Fig. 1a**). Because of the presence of multiple putative OGT-target sites in the poly(S/T) region in DELLA proteins, SPY has long been hypothesized to O-GlcNAcylate DELLAs[5,15]. We have recently shown by MS analysis that the *Arabidopsis* DELLA protein RGA is indeed O-GlcNAcylated[20]. However, SEC is the OGT catalyzing this modification, whereas SPY is not required. Intriguingly, mutant analysis has indicated that SEC and SPY play opposite roles in GA signaling, in which SEC is a positive regulator, and SPY is a negative regulator[20,21]; however, the biochemical function of SPY remains unsolved.

In this report, through sensitive MS analysis and *in vitro* enzyme assays, we uncovered the biochemical function of SPY as a novel protein *O*-fucosyltransferase, which modifies the *Arabidopsis* DELLA protein RGA by attaching monofucose to specific serine and threonine residues. Importantly, this unusual O-fucosylation enhances DELLA activity by promoting DELLA binding to key transcription factors in BR and light-signaling pathways. Our results revealed that SPY-dependent O-fucosylation plays an important role in modulating plant development by regulating activities of nuclear transcription factors. Our findings have broader implications because SPY orthologs are conserved in diverse organisms[17], although their biochemical functions remain to be characterized.

RESULTS

RGA shows SPY-dependent O-fucosylation *in planta*

A major advance in uncovering SPY function came from our close interrogation of the liquid chromatography (LC)–electron transfer dissociation (ETD)–MS/MS spectrum of FLAG-tagged RGA isolated from P_{RGA}:*FLAG-RGA* transgenic *Arabidopsis* expressing FLAG-tagged RGA under control of the *RGA* promoter. In this experiment, FLAG-RGA was affinity-purified from *Arabidopsis* and digested with the endoproteinase trypsin, then subjected to LC–ETD–MS/MS analyses. We discovered a novel post-translational modification, mono *O*-fucose, attached to specific serine and threonine residues in RGA (**Fig. 1a**,**b** and **Supplementary Note 1**); O-fucosylation of serine or threonine residues has not been identified in nuclear proteins. Unexpectedly, we found that O-fucosylation levels in RGA were decreased in *spy-8* but were unaffected by *sec-3* (**Fig. 1b**), thus suggesting that SPY directly or indirectly promotes O-fucosylation of RGA. However, we detected only very low levels of O-fucosylation in RGA from purified *Arabidopsis* samples, possibly because this type of modification is easily lost during purification and MS analysis.

To further examine the role of SPY in O-fucosylation of RGA, we transiently expressed the FLAG-RGA^{GKG} mutant alone,

[1]Department of Biology, Duke University, Durham, North Carolina, USA. [2]Department of Chemistry, University of Virginia, Charlottesville, Virginia, USA. [3]Department of Biochemistry, Duke University Medical Center, Durham, North Carolina, USA. [4]Department of Plant Biology, University of Minnesota, Saint Paul, Minnesota, USA. [5]Department of Chemistry, Duke University, Durham, North Carolina, USA. [6]Department of Pathology, University of Virginia, Charlottesville, Virginia, USA. [7]These authors contributed equally to this work. *e-mail: tps@duke.edu

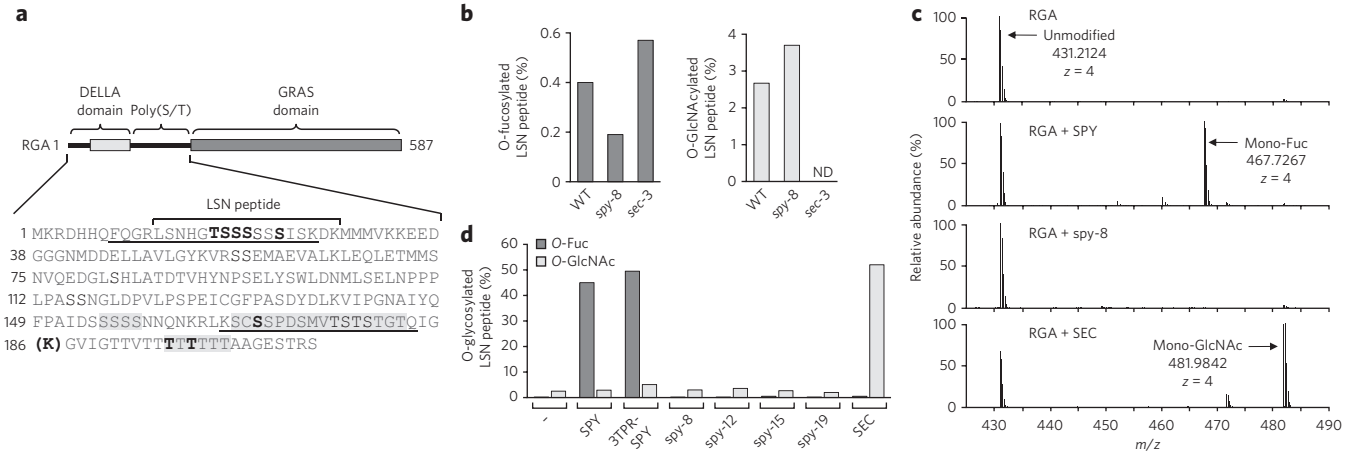

Figure 1 | RGA shows SPY-dependent O-fucosylation *in planta*. (**a**) O-fucosylation sites in RGA. In RGA schematic (top), solid lines indicate two structurally disordered regions. The sequences of the DELLA domain and poly(S/T) region are shown below the schematic. The LSN peptide was mono-O-fucosylated in FLAG-RGA from transgenic *Arabidopsis*. Additional O-fucosylation sites were identified with FLAG-RGA^{GKG} from tobacco that was coexpressed with SPY. Boldface S/T indicates modification sites confirmed by MS/MS. Sequences shaded in gray contain one or more additional unmapped sites (detailed information in **Supplementary Table 1**). The boldface K in parentheses indicates the extra lysine residue in RGA^{GKG}. RGA^{pep1} and RGA^{pep2} are underlined. (**b**) LC–ETD–MS/MS analysis showing that O-fucosylation levels in the RGA LSN peptide decreased in *spy-8* plants compared with WT and *sec-3* plants. ND, not detected. (**c**) MS^1 spectra of the RGA LSN peptide from tobacco expressing FLAG-RGA^{GKG} either alone (RGA) or with SPY, spy-8 or SEC. Unmodified peptide, predicted *m/z* = 431.2130. Mono-O-fucosylated RGA peptide (mono-Fuc; predicted *m/z* = 467.7195) was detected in only RGA + SPY, whereas mono-O-GlcNAcylated peptide (predicted *m/z* = 481.9823) was detected in only RGA + SEC. (**d**) MS analysis showing that O-fucosylation levels in the RGA LSN peptide were dramatically increased only under coexpression with SPY or 3TPR-SPY. Protein samples from four independent coexpression experiments for WT SPY and SEC, and two independent coexpression experiments for mutant spy proteins were analyzed and yielded similar results. Immunoblots showed similar ratios of SPY or mutant spy versus FLAG-RGA^{GKG} in tobacco protein extracts (**Supplementary Fig. 2**).

or coexpressed it with Myc-SPY (RGA + SPY) or Myc-SEC (RGA + SEC, control), in tobacco leaves by agroinfiltration. RGA^{GKG} contains an extra lysine residue between G185 and G186 in RGA (**Fig. 1a**), thereby creating an additional trypsin-cleavage site and facilitating the detection of the O-fucosylated peptide that spans the poly(T) tract within the poly(S/T) region. Collisionally activated dissociation (CAD)– and ETD–MS/MS analyses showed that the purified FLAG-RGA^{GKG} from the RGA + SPY samples was highly O-fucosylated (**Fig. 1c**,**d**, **Supplementary Fig. 2** and **Supplementary Notes 2**–**5**). One of the most abundant O-fucosylated sequences was located in the LSN peptide, which was also O-fucosylated in *Arabidopsis* (**Fig. 1a**,**c**,**d** and **Supplementary Table 1**). Other major O-fucosylation sites were within the poly(T) tract (**Fig. 1a** and **Supplementary Table 1**). In total, a minimum of nine O-fucosylation sites in four RGA peptides were identified, and eight of these sites mapped to specific serine or threonine residues (**Fig. 1a**, **Supplementary Table 1** and **Supplementary Notes 1**–**5**). In contrast, the RGA-alone samples showed very low amounts of O-fucosylation compared with that in the RGA + SPY samples (**Fig. 1c**,**d** and **Supplementary Table 1**), thus indicating that RGA was modified to a lesser extent by endogenous protein *O*-fucosyltransferase activity in tobacco. Coexpression of the spy-8 mutant protein or SEC did not increase O-fucosylation in RGA. These results indicated that SPY promotes O-fucosylation of RGA. To investigate whether SPY also promotes O-fucosylation of other *A. thaliana* (At) DELLAs, we performed MS analysis of purified GAI, RGL1 and RGL2, which were coexpressed with SPY in tobacco. We identified an O-fucosylated peptide near the N terminus (9-ESSAGEGGSSSMTTVIK-25) of RGL1 (**Supplementary Fig. 3**).

SPY is a novel protein *O*-fucosyltransferase

Our RGA and SPY coexpression experiments using the tobacco system strongly suggested that SPY is a novel protein *O*-fucosyltransferase (POFUT) that modifies RGA. Protein *O*-fucosyltransferases modify target proteins (the acceptor substrates) by transferring *O*-fucose from GDP–fucose (the donor substrate) to the hydroxy oxygen of serine and threonine residues. In fact, protein O-fucosylation is rare and is known to occur primarily in the endoplasmic reticulum (ER) and to promote protein folding and/or ligand binding of several cell-surface transmembrane proteins[22], for example, epidermal growth factor domain–containing Notch family proteins[23] and thrombospondin type 1 repeats[24]. The O-fucosylation of epidermal growth factor domains and thrombospondin type 1 repeats is catalyzed by ER-localized POFUT1 and POFUT2, respectively[22]. POFUT1 and POFUT2 have similar 3D structures with two β/α/β Rossmann-like folds (GT-B folds)[25,26] but are distinct from the structures of OGTs[27] (**Supplementary Fig. 1b**,**c**).

To assess whether SPY directly O-fucosylates RGA, we performed *in vitro* enzyme assays, using two synthetic RGA peptides that were O-fucosylated *in planta* (**Fig. 1a** and **Supplementary Table 1**) as the acceptor substrates. Purified recombinant 3TPR-SPY protein (**Supplementary Fig. 4a**), which is truncated by eight TPRs from the N terminus, was used in the enzyme assays. This truncated 3TPR-SPY was equally active as the full-length SPY (FL-SPY) in our tobacco assay (**Fig. 1d** and **Supplementary Table 1**), in agreement with results from a previous report showing that truncated human OGT containing only five TPRs has enzymatic activity similar to that of the full-length protein[28]. In addition, we obtained larger amounts of soluble 3TPR-SPY than FL-SPY in an *Escherichia coli* expression system. In the initial enzyme assays, each RGA peptide was incubated with GDP–fucose and purified 3TPR-SPY in various buffer conditions for 2 h and was then analyzed by MALDI–MS. 88% of RGA peptide 1 (RGA^{pep1}) was mono-fucosylated in the presence of both GDP–fucose and 3TPR-SPY, but no modification was detected in the absence of GDP–fucose or SPY (**Fig. 2a**), thus demonstrating that SPY is indeed a POFUT that modifies RGA. Peptide 2 (RGA^{pep2}) was also O-fucosylated by SPY, although it was modified at much lower levels than those in RGA^{pep1}

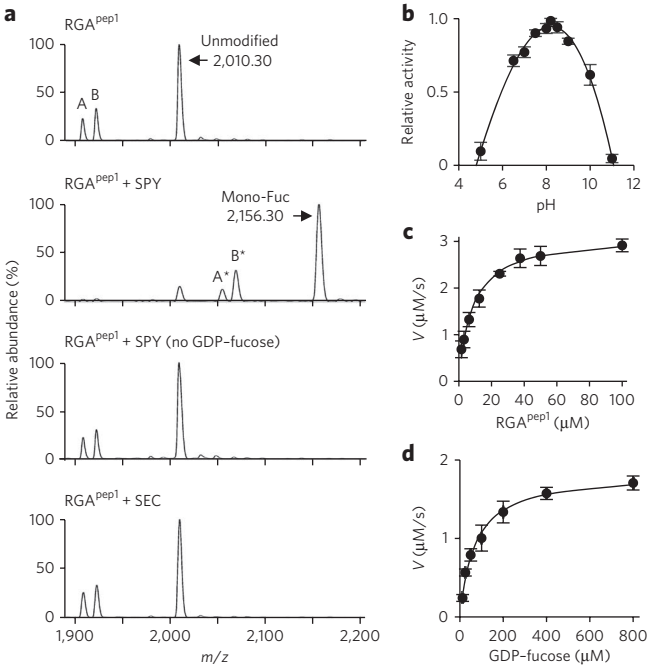

Figure 2 | SPY is a novel protein O-fucosyltransferase (POFUT). (**a**) MALDI-MS spectra of the RGA peptide 1 (RGA^{pep1}) from *in vitro* enzyme assays ± 3TPR-SPY or GDP-fucose or SEC. Monofucosylated RGA^{pep1} (predicted *m/z* = 2,155.17 versus 2,009.11 for unmodified peptide) was detected in only RGA + 3TPR-SPY in the presence of GDP-fucose. Peaks labeled A and B (observed *m/z* = 1,908.92 for A; 1,923.17 for B) are unmodified incomplete peptides (by-products of RGA^{pep1} synthesis) with a T or S deletion, respectively. Peaks labeled A* and B* are monofucosylated A and B peptides (observed *m/z* = 2,054.98 for A*; 2,069.23 for B*). Reactions with three batches of purified enzyme were analyzed and yielded similar results. (**b**) Optimal pH for SPY *in vitro* enzyme assay determined by malachite green-coupled assay. (**c**,**d**) Steady-state kinetics determined for 3TPR-SPY with malachite green-coupled assays. *V*, velocity. In **c**, the GDP-fucose concentration was fixed at 800 μM. In **d**, the RGA^{pep1} concentration was fixed at 312.5 μM. In **b**–**d**, each data point is the average of three independent experiments (with two technical repeats each). Means ± s.e.m. are shown. The K_m for each substrate was calculated with Lineweaver-Burk plots (**Supplementary Fig. 6a**,**b**).

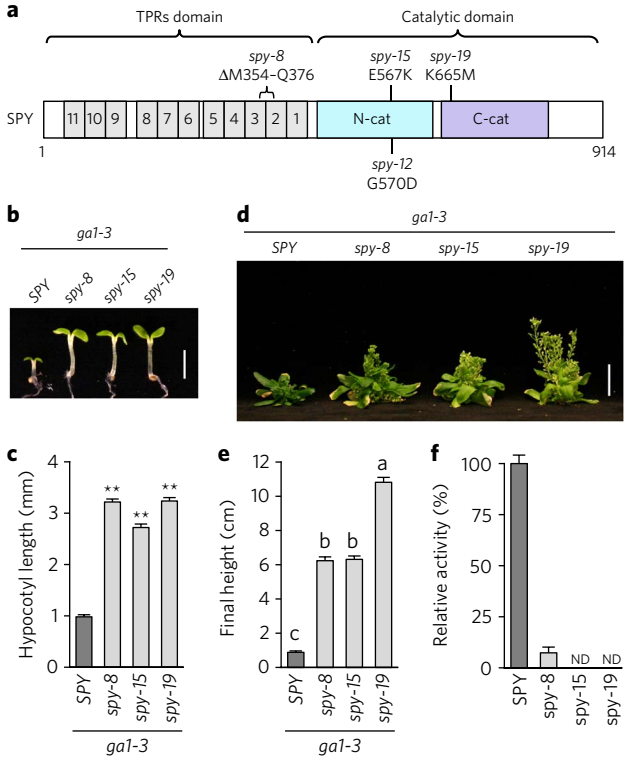

Figure 3 | Phenotype and enzyme-activity analyses of the spy mutants. (**a**) Schematic of SPY protein structure. Mutation in spy-8 is located in TPR2-3, whereas mutations in spy-12, spy-15 and spy-19 are located in the C-terminal catalytic domain (C-cat). N-cat, N-terminal catalytic domain. (**b**,**c**) All *spy* alleles rescued the hypocotyl growth defect of the GA-deficient mutant *ga1-3*. Hypocotyl lengths of 6-d-old seedlings grown in short-day conditions were measured. In **b**, scale bar, 2.5 mm. In **c**, average hypocotyl lengths are shown as means ± s.e.m. (n = 20 seedlings). $^{**}P < 0.01$ compared with WT, determined by two-tailed Student's *t* test. Three independent experiments were analyzed with similar results. (**d**) Photograph of 67-d-old plants. Scale bar, 2 cm. (**e**) Average final heights of *ga1-3* and *ga1-3 spy* mutants. The data are shown as means ± s.e.m. (n = 13 plants). Statistical analyses were performed with two-tailed Student's *t* tests. Different letters above the bars indicate significant differences, $P < 0.01$. Two independent experiments were analyzed and yielded similar results. In **d**,**e**, plants were grown under 16 h-light conditions. (**f**) Malachite green-coupled assay showing that spy-8 retains low POFUT activity, but no activity was detected for spy-15 or spy-19. The indicated truncated 3TPR-SPY and spy-mutant proteins were expressed and purified as decahistidine-maltose-binding protein fusion proteins for this assay, and RGA^{pep1} and GDP-fucose were used as substrates. Means ± s.e.m. of three independent experiments (with two technical repeats each) are shown. ND, not detected. The immunoblot detected by anti-SPY antibodies indicates that similar amounts of WT and mutant enzymes were used in the assays (**Supplementary Fig. 8a**).

(**Supplementary Fig. 4b**). Therefore, RGA^{pep1} was used for further SPY enzyme characterization.

To analyze the donor-substrate specificity of SPY, four other nucleotide sugars were tested. These included UDP–GlcNAc (donor substrate for OGT), GDP–mannose, UDP–galactose and UDP-glucose. By MALDI–MS analysis, we found that SPY did not exhibit any activity in the presence of these four nucleotide sugars, thus indicating that SPY displays specific POFUT activity. In addition, our *in vitro* assay using RGA peptides showed that SEC had only OGT activity (**Supplementary Fig. 5a**,**b**) but no POFUT activity (**Fig. 2a**), in agreement with the results of our RGA + SEC coexpression study with the tobacco system (**Fig. 1c**,**d**).

For further characterization of the POFUT activity of SPY, we used malachite green–coupled reaction[29], a recently developed method for assaying glycosyltransferase activities, because this assay is more efficient than MALDI–MS. In this assay, the glycosyltransferase reaction is coupled with a phosphatase (ectonucleoside triphosphate diphosphohydrolase) that releases the β-phosphate of GDP, which is then detected by the malachite green reagents[29,30]. Using this assay, we found that SPY enzyme activity was not significantly affected by salt concentration or metal cations (**Supplementary Fig. 6a**,**b**) but was sensitive to pH, exhibiting maximal activity at pH 8.2 (**Fig. 2b**). Michaelis–Menten kinetics analysis was then performed under the optimized buffer conditions (50 mM Tris, pH 8.2, 5 mM $MgCl_2$ and 50 mM NaCl). The O-fucosylation reaction has two substrates: RGA^{pep1} and GDP–fucose. To simplify the kinetics analysis, two sets of reactions were performed, one with a fixed GDP–fucose concentration at 800 μM and the other with a fixed peptide concentration at 312.5 μM (**Fig. 2c**,**d**). For 3TPR-SPY, the K_m for RGA^{pep1} was 8.23 ± 0.10 μM (mean ± s.e.), with a k_{cat} of 0.50 ± 0.02 s^{-1}. The K_m for GDP–fucose was determined to be 50.48 ± 3.90 μM, with a k_{cat} of 0.27 ± 0.01 s^{-1} (**Supplementary Fig. 7a**,**b**).

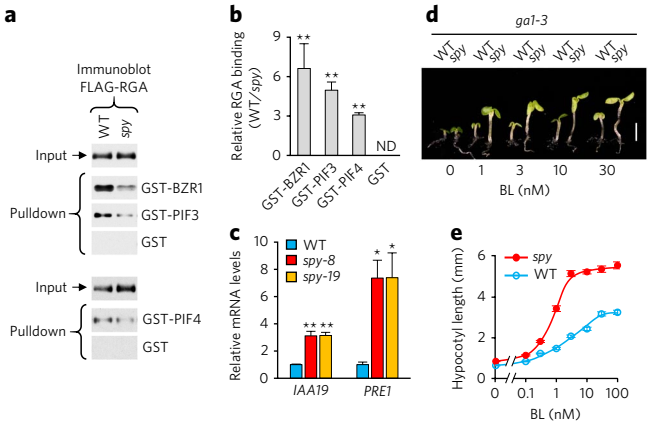

Figure 4 | O-fucosylation enhances RGA activity by promoting RGA binding to its interactors. (**a**) *In vitro* pulldown assay. Recombinant GST, GST-BZR1, GST-PIF3 and GST-PIF4 bound to glutathione–Sepharose beads were used separately to pull down FLAG-RGA from protein extracts from *Arabidopsis* in a WT *SPY* or *spy-8* background. Immunoblots containing input *Arabidopsis* extracts and samples pulled down with FLAG-RGA were detected with an anti-FLAG antibody. Full blot images are shown in **Supplementary Figure 12**. Ponceau S–stained blots indicated that similar amounts of the GST/GST-fusion proteins were used in each pair of the pulldown assays (**Supplementary Fig. 8b**). (**b**) Relative binding of FLAG-RGA (from WT versus *spy* background) to GST-fusion proteins. Data are means ± s.e.m. of three independent experiments. $^{**}P < 0.01$ by two-tailed Student's *t* test. (**c**) RT-qPCR analysis showing that transcript levels of *IAA19* and *PRE1* (common target genes of BZR1, PIF and DELLA) were increased in *spy-8* and *spy-19* mutants compared with WT (all in the *ga1-3* background). *PP2A* was used to normalize samples. Data are means ± s.e.m. of three independent samples and two technical repeats each. $^{*}P < 0.05$; $^{**}P < 0.01$ by two-tailed Student's *t* tests. (**d**,**e**) *spy-8*, compared with WT *SPY*, conferred an elevated BR response in hypocotyl growth. The *ga1-3* and *spy-8 ga1-3* seedlings (labeled as WT and *spy-8*) were grown in medium containing 2 μM propiconazole (a BR-biosynthesis inhibitor) and varying concentrations of brassinolide (BL). Hypocotyl lengths were measured at day 6 ($n = 20$ seedlings). Scale bar in **d**, 2.5 mm. Average hypocotyl lengths in **e** are means ± s.e.m.

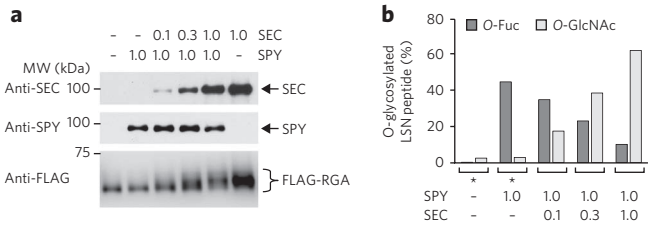

Figure 5 | SPY and SEC compete with each other in reciprocal modifications of RGA. (**a**) Immunoblots showing fixed amounts of SPY and increasing levels of SEC in tobacco extracts coexpressing FLAG-RGA. The blots were probed with anti-SEC, anti-SPY or anti-FLAG antibodies. Tobacco agroinfiltrations used mixed agrobacterium cultures containing FLAG-RGA^{GKG} and/or Myc-SPY and/or Myc-SEC constructs (0.1×, optical density at 600 nm (OD_{600}) of 0.06; 0.3×, OD_{600} of 0.2; 1×, OD_{600} of 0.6). The decrease in FLAG-RGA mobility correlated with increasing amounts of coexpressed SEC, owing to greater numbers of GlcNAcylated residues in FLAG-RGA. Full blot images are shown in **Supplementary Figure 12**. MW, molecular weight. (**b**) MS analysis showing that increasing expression of SEC results in elevated O-GlcNAcylation but is inversely correlated with O-fucosylation levels in the RGA LSN peptide. Peptide abundances were calculated from MS^1 ion currents integrated across the chromatographic elution of peptides. Asterisk, MS data from **Figure 1d**, included for comparison.

spy alleles define key residues for POFUT activity

Previous studies have identified a number of hypomorphic *spy* alleles, some located in the TPR domain and others located in the C-terminal catalytic domain[15] (**Fig. 3a**). For example, the spy-8 protein contains an in-frame 23–amino acid deletion (M354–Q376 (ref. 15)) in TPR3–TPR2, whereas spy-12 (G570D[15]), spy-15 (E567K[15]) and spy-19 (K665M, identified in this study) each contain a single amino acid substitution in the catalytic domain. Previous phenotype characterization of the single *spy* mutants has shown that *spy-12*, *spy-15* and *spy-19* display more severe fertility defects and earlier flowering time than *spy-8*, thus indicating that these catalytic-domain mutations are stronger alleles than *spy-8* (ref. 15). To investigate the specific effects of *spy* alleles on GA signaling, we analyzed phenotypes of *spy* mutants in the GA-deficient-mutant *ga1-3* background. At the seedling stage, *spy-8* rescued the hypocotyl growth of *ga1-3* to a similar extent as that observed in *spy-15* and *spy-19* mutants (**Fig. 3b**,**c**). However, at the adult stage, *spy-19* rescued the stem growth defect of *ga1-3* more efficiently than did *spy-8* and *spy-15* (**Fig. 3d**,**e**). To test whether spy-8 protein (with mutations in the TPR region) still retained some catalytic activity, we expressed and purified spy-8, spy-15 and spy-19 mutant proteins (3TPR-SPY truncated versions) and performed *in vitro* enzyme assays. Malachite green–coupled assays showed that the POFUT activity of spy-8 was 7.3% that of the wild type (WT), whereas no activity was detected for spy-15 or spy-19 (**Fig. 3f** and **Supplementary Fig. 8a**). To detect the residual enzymatic activities of spy-15 and spy-19, we performed *in vitro* enzyme assays with a 16-h incubation time, then performed MALDI–MS. The results of this assay were consistent with those of the malachite green assay with spy-8, showing a low POFUT activity (8.5% that of WT), whereas spy-15 and spy-19 did not exhibit any POFUT activity (**Supplementary Fig. 9**). Similar results were also observed when these spy-mutant proteins (plus spy-12) were coexpressed with FLAG-RGA^{GKG} in tobacco, although no residual POFUT activity was detected for spy-8 (**Fig. 1d**). These results indicated that E567, G570 and K665 are essential for the POFUT activity of SPY, and TPR2 and TPR3 (partially deleted in spy-8) also play an important role in SPY function. These results confirmed that SPY is a novel POFUT, although its paralog SEC is an OGT.

3D structure modeling based on the human (Hs) OGT crystal structure[31] predicted that SPY and SEC fold similarly to HsOGT (**Supplementary Fig. 1b**,**d**,**e**). K665 in SPY (mutated in spy-19) is absolutely conserved in all OGT and SPY-like sequences (**Supplementary Fig. 10b**) and is equivalent to K842 in HsOGT, which binds the β-phosphate of UDP–GlcNAc and is critical for OGT activity[27,32,33]. It is possible that K665 in SPY may serve a similar function as K842 in HsOGT by interacting with the β-phosphate of GDP–fucose and helping to position this nucleotide sugar in its substrate-binding pocket. E567 and G570 in SPY (mutated in spy-15 and spy-12, respectively) are also highly conserved in almost all OGT and SPY-like sequences (**Supplementary Fig. 10a**). However, the transition helix (H3, between the TPRs and catalytic domain) and the first two helices (H1 and H2) of the N-terminal catalytic domain, which are important for the catalytic activity of HsOGT, are more divergent in SPY (**Supplementary Fig. 1b**,**e** and **Supplementary Fig. 10a**). Most notably, two key residues (H498 and H499 in HsOGT, and F540 and H541 in AtSEC), which are important for OGT activity[20,27,32,33], are absent in SPY. These differences may contribute to the distinct enzymatic activity of SPY.

O-fucosylation promotes RGA binding with its interactors

Previously, we have shown that the *spy* mutation does not promote RGA degradation or affect RGA nuclear localization[15]. One possible role of RGA O-fucosylation by SPY is regulation of binding affinity

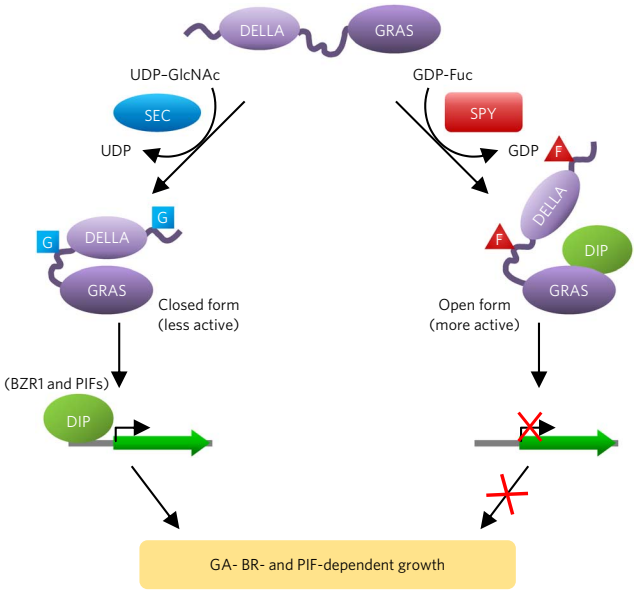

Figure 6 | Model of the role of O-fucosylation versus O-GlcNAcylation of RGA. O-fucosylation (F) by SPY may induce RGA to adopt an open conformation that is a more active growth repressor; this open form promotes binding of the RGA GRAS domain to interacting transcription factors (for example, BZR1 and PIFs), thus leading to downregulated expression of target genes of BZR1 and PIFs and restriction of plant growth. In contrast, O-GlcNAcylation (G) by SEC may cause RGA to fold into a closed conformation that is less active, because this form decreases the binding affinity of RGA to BZR1 and PIFs, thus allowing growth-related target genes to be activated. DIP, DELLA-interacting protein.

between RGA and its interacting transcription factors, a major regulatory mechanism in DELLA-modulated plant development[6–8]. Recent studies have shown that BRZ1 (a BR-signaling activator) and PIFs (light-signaling regulators) are key transcription factors promoting hypocotyl elongation in response to BR and light conditions, and that DELLAs inhibit hypocotyl growth by interacting with BZR1 and PIFs and consequently repressing expression of BZR1- and PIF-induced genes[6,7,34]. To test the effect of *spy* on DELLA interaction with BZR1 and PIFs, an *in vitro* pulldown assay was performed with *Arabidopsis* protein extracts of P_{RGA}:*FLAG-RGA* transgenic lines in the WT *SPY* or the *spy-8* background, and three recombinant RGA-interacting proteins, BZR1, PIF3 and PIF4, which were expressed individually in *E. coli* as glutathione *S*-transferase (GST)-fusion proteins. GST was also included as a negative control. We found that FLAG-RGA (O-fucosylated) from WT displayed stronger binding to GST-BZR1, GST-PIF3 and GST-PIF4 than did FLAG-RGA (less fucosylated) from the *spy-8* mutant (**Fig. 4a**,**b** and **Supplementary Fig. 8b**). These results suggested that O-fucosylation of RGA by SPY increases RGA activity by enhancing RGA interactions with BZR1 and PIFs. This model predicts that *spy* mutations should upregulate the expression of DELLA-repressed and BZR1- and PIF-induced genes, thus leading to increased BR- and PIF-dependent responses. *INDOLE 3-ACETIC ACID INDUCIBLE19* (*IAA19*) and *PACLOBUTRAZOL RESISTANCE1* (*PRE1*) are two common target genes of BZR1, PIFs and DELLAs[34–36]. RT–qPCR analysis showed that transcript levels of *IAA19* and *PRE1* were upregulated by *spy-8* and *spy-19* (**Fig. 4c**). We also found that *ga1-3 spy* seedlings had longer hypocotyls than those of *ga1-3* seedlings (**Fig. 3b**,**c**), an effect known to be promoted by PIF3, PIF4 and PIF5 (refs. 37,38). Moreover, in the presence of a BR-biosynthesis inhibitor, *spy-8* enhanced the BR response in hypocotyl elongation (**Fig. 4d**,**e**). These results indicated that SPY negatively regulates GA-, BR- and PIF-dependent pathways by O-fucosylating RGA and enhancing its activity.

We have previously shown that, in contrast to the role of SPY in activating RGA, O-GlcNAcylation of RGA by SEC decreases RGA activity through interfering with RGA-BZR1 and RGA-PIF interactions[20]. Interestingly, the sites of O-fucosylation in RGA largely overlap with the sites of O-GlcNAcylation within the two structurally disordered regions: the LSN peptide near the N terminus and the poly(S/T) region[20] (**Fig. 1a** and **Supplementary Fig. 11a**). To test whether SPY and SEC compete with each other in modifying RGA, we transiently expressed FLAG-RGA together with a fixed amount of SPY and varying amounts of SEC in tobacco (**Fig. 5**). FLAG-RGA was then purified and analyzed by immunoblotting and LC–ETD–MS/MS. Increasing ratios of SEC to SPY correlated with slower gel mobility of FLAG-RGA (**Fig. 5a**), owing to elevated O-GlcNAcylation[20]. MS analysis further showed that increasing levels of SEC led to decreased O-fucosylation and elevated O-GlcNAcylation in the RGA LSN peptide (**Fig. 5b**), thus supporting the notion that SPY and SEC compete with each other in regulating RGA activity by reciprocal modifications.

DISCUSSION

Our study discovered the novel O-fucosylation of nuclear DELLA repressor by SPY in *Arabidopsis*. Sequence comparison and 3D structure prediction indicated that SPY is highly similar to the TPR-containing OGTs[17] (**Supplementary Figs. 1** and **10**). This similarity to the animal OGTs has led to the longstanding hypothesis that SPY functions as an OGT[17]. However, results of previous enzymatic assays have been inconclusive. Here, we showed that SPY is an unusual POFUT and is unrelated to the ER-localized POFUTs that modify secreted cell-surface proteins in animals[22]. We further showed that SPY-dependent O-fucosylation enhances DELLA activity, a function opposite from the role of SEC as an inhibitor of DELLA by O-GlcNAcylation. In addition, SPY and SEC competed with each other in modifying RGA in transient coexpression assays in tobacco. We propose that O-GlcNAcylation may stabilize RGA in a 'closed form', whereas O-fucosylation may induce a conformational transition of RGA to an 'open form' (**Fig. 6**). The O-GlcNAcylated closed form of RGA is a less active growth repressor, because this conformation prevents interaction with DELLA-interacting proteins (DIPs, such as BZR1 and PIFs), whereas the O-fucosylated open form of RGA is a more active growth repressor, because its GRAS domain can bind DIPs efficiently.

The sites of O-fucosylation and O-GlcNAcylation in RGA are clustered within two regions: the LSN peptide near the N terminus and the poly(S/T) region[20] (**Fig. 1a** and **Supplementary Fig. 11a**). These two regions in RGA are structurally disordered, and the sequences surrounding the glycosylation sites are not conserved among the five AtDELLAs (RGA, GAI, RGL1, RGL2 and RGL3; **Supplementary Fig. 11a**,**b**). Nonetheless, coexpression of SEC with each AtDELLA in the tobacco system resulted in slower gel mobility of these AtDELLAs, thus supporting that SEC O-GlcNAcylates all AtDELLAs[20]. To investigate whether SPY also modifies the other AtDELLAs, MS analysis was performed, because O-fucosylation of RGA did not cause a visible gel mobility shift[20] (**Supplementary Fig. 2**). Our initial analysis showed that RGL1 is O-fucosylated by SPY (**Supplementary Fig. 3**). These results indicate that, in addition to RGA, SEC and SPY also glycosylate and regulate the activities of at least some of the other AtDELLAs. This idea is supported by the dramatically longer hypocotyl and taller final height of the *ga1 rga spy* triple mutant compared with the *ga1 rga* double mutant[39]. Our results also suggest that SEC and SPY may modify the flexible regions of target proteins by interacting with the substrate amide backbone, similarly to HsOGT[27].

The truncated 3TPR-SPY, which lacks TPR4–11, was as active as FL-SPY in modifying RGA after overexpression in tobacco. However, TPR4–11 of SPY may be important for SPY's function *in vivo*, for example, in recruiting target proteins and/or forming

protein complexes with its interactors. This idea could be tested by expression of *3TPR-SPY* under the control of the *SPY* promoter in the *spy*-mutant background. Among several *spy* alleles with mutations either in TPR2-3 (*spy-8*) or in the catalytic domain (*spy-12*, *spy-15* and *spy-19*), we found that *spy-19* (K665M) displayed a more severe phenotype at the adult stage, although all *spy* alleles tested showed similar hypocotyl phenotypes at the seedling stage (**Fig. 3b–e**). The elevated GA signaling caused by the leaky *spy-8* might already have saturated the GA response for hypocotyl growth, and therefore no differences were observed for this phenotype and expression of corresponding growth-related genes (*IAA19* and *PRE1*) among the different *spy* mutants. In contrast, inflorescence stem growth may require higher GA signaling activities to reach a saturated GA response.

OGT-mediated protein O-GlcNAcylation has been extensively studied in animals and plays a key role in regulating a plethora of intracellular signaling events in response to nutrient and stress status[40,41]. In plants, O-fucosylation and O-GlcNAcylation are likely to play important roles in regulating multiple intracellular processes. The *spy* mutants display pleiotropic phenotypes, some of which (for example, fused cotyledons and altered phyllotaxy) are unrelated to GA responses[15]. Previous genetic studies have further shown that SPY promotes phytohormone cytokinin signaling[42] and regulates circadian rhythms[43]. Our studies indicated that SPY and SEC play opposite roles in regulating DELLA activity. Intriguingly, *spy sec* double mutations confer an embryonic-lethal phenotype[18]. The impaired embryogenesis of the *spy sec* double mutant is probably due to defects in other pathways that are not directly related to GA signaling. O-GlcNAcylation in animals affects many fundamentally important cellular functions, including epigenetic regulation of chromatin structure, transcription, translation and protein degradation[40,41]. If O-GlcNAcylation and O-fucosylation also modulate these processes in plants, disruption of multiple cellular functions and pathways in the *spy sec* double mutant would be deleterious to the developing embryo. Interestingly, SPY-like genes are absent in animals but are present in diverse organisms including prokaryotes, protists, algae and all plants[17], although their biochemical functions have not been well characterized. These conserved SPY orthologs in other organisms may have POFUT activity or other novel glycosyltransferase activities that are distinct from those of OGTs. Future studies should reveal the roles of intracellular protein O-fucosylation in regulating developmental processes in diverse organisms.

Received 4 August 2016; accepted 1 December 2016;
published online 28 February 2017

METHODS

Methods, including statements of data availability and any associated accession codes and references, are available in the online version of the paper.

References

1. Vert, G. & Chory, J. Crosstalk in cellular signaling: background noise or the real thing? *Dev. Cell* **21**, 985–991 (2011).
2. Silverstone, A.L., Ciampaglio, C.N. & Sun, T. The *Arabidopsis RGA* gene encodes a transcriptional regulator repressing the gibberellin signal transduction pathway. *Plant Cell* **10**, 155–169 (1998).
3. Peng, J. *et al.* The *Arabidopsis* GAI gene defines a signaling pathway that negatively regulates gibberellin responses. *Genes Dev.* **11**, 3194–3205 (1997).
4. Sun, T.P. The molecular mechanism and evolution of the GA-GID1-DELLA signaling module in plants. *Curr. Biol.* **21**, R338–R345 (2011).
5. Davière, J.M. & Achard, P. Gibberellin signaling in plants. *Development* **140**, 1147–1151 (2013).
6. de Lucas, M. *et al.* A molecular framework for light and gibberellin control of cell elongation. *Nature* **451**, 480–484 (2008).
7. Feng, S. *et al.* Coordinated regulation of *Arabidopsis thaliana* development by light and gibberellins. *Nature* **451**, 475–479 (2008).
8. Xu, H., Liu, Q., Yao, T. & Fu, X. Shedding light on integrative GA signaling. *Curr. Opin. Plant Biol.* **21**, 89–95 (2014).
9. Ueguchi-Tanaka, M. *et al. GIBBERELLIN INSENSITIVE DWARF1* encodes a soluble receptor for gibberellin. *Nature* **437**, 693–698 (2005).
10. Murase, K., Hirano, Y., Sun, T.P. & Hakoshima, T. Gibberellin-induced DELLA recognition by the gibberellin receptor GID1. *Nature* **456**, 459–463 (2008).
11. McGinnis, K.M. *et al.* The *Arabidopsis SLEEPY1* gene encodes a putative F-box subunit of an SCF E3 ubiquitin ligase. *Plant Cell* **15**, 1120–1130 (2003).
12. Sasaki, A. *et al.* Accumulation of phosphorylated repressor for gibberellin signaling in an F-box mutant. *Science* **299**, 1896–1898 (2003).
13. Griffiths, J. *et al.* Genetic characterization and functional analysis of the GID1 gibberellin receptors in *Arabidopsis*. *Plant Cell* **18**, 3399–3414 (2006).
14. Dill, A., Jung, H.-S. & Sun, T.P. The DELLA motif is essential for gibberellin-induced degradation of RGA. *Proc. Natl. Acad. Sci. USA* **98**, 14162–14167 (2001).
15. Silverstone, A.L. *et al.* Functional analysis of SPINDLY in gibberellin signaling in *Arabidopsis*. *Plant Physiol.* **143**, 987–1000 (2007).
16. Wilson, R.N. & Somerville, C.R. Phenotypic suppression of the gibberellin-insensitive mutant (*gai*) of *Arabidopsis*. *Plant Physiol.* **108**, 495–502 (1995).
17. Olszewski, N.E., West, C.M., Sassi, S.O. & Hartweck, L.M. *O*-GlcNAc protein modification in plants: evolution and function. *Biochim. Biophys. Acta* **1800**, 49–56 (2010).
18. Hartweck, L.M., Scott, C.L. & Olszewski, N.E. Two *O*-linked *N*-acetylglucosamine transferase genes of *Arabidopsis thaliana* L. Heynh. have overlapping functions necessary for gamete and seed development. *Genetics* **161**, 1279–1291 (2002).
19. Jacobsen, S.E., Binkowski, K.A. & Olszewski, N.E. SPINDLY, a tetratricopeptide repeat protein involved in gibberellin signal transduction in *Arabidopsis*. *Proc. Natl. Acad. Sci. USA* **93**, 9292–9296 (1996).
20. Zentella, R. *et al.* *O*-GlcNAcylation of master growth repressor DELLA by SECRET AGENT modulates multiple signaling pathways in *Arabidopsis*. *Genes Dev.* **30**, 164–176 (2016).
21. Jacobsen, S.E. & Olszewski, N.E. Mutations at the *SPINDLY* locus of *Arabidopsis* alter gibberellin signal transduction. *Plant Cell* **5**, 887–896 (1993).
22. Luther, K.B. & Haltiwanger, R.S. Role of unusual O-glycans in intercellular signaling. *Int. J. Biochem. Cell Biol.* **41**, 1011–1024 (2009).
23. Okajima, T. & Irvine, K.D. Regulation of notch signaling by O-linked fucose. *Cell* **111**, 893–904 (2002).
24. Hofsteenge, J. *et al.* C-mannosylation and O-fucosylation of the thrombospondin type 1 module. *J. Biol. Chem.* **276**, 6485–6498 (2001).
25. Lira-Navarrete, E. *et al.* Structural insights into the mechanism of protein O-fucosylation. *PLoS One* **6**, e25365 (2011).
26. Chen, C.I. *et al.* Structure of human POFUT2: insights into thrombospondin type 1 repeat fold and O-fucosylation. *EMBO J.* **31**, 3183–3197 (2012).
27. Lazarus, M.B., Nam, Y., Jiang, J., Sliz, P. & Walker, S. Structure of human *O*-GlcNAc transferase and its complex with a peptide substrate. *Nature* **469**, 564–567 (2011).
28. Kreppel, L.K. & Hart, G.W. Regulation of a cytosolic and nuclear O-GlcNAc transferase: role of the tetratricopeptide repeats. *J. Biol. Chem.* **274**, 32015–32022 (1999).
29. Wu, Z.L., Ethen, C.M., Prather, B., Machacek, M. & Jiang, W. Universal phosphatase-coupled glycosyltransferase assay. *Glycobiology* **21**, 727–733 (2011).
30. Baykov, A.A., Evtushenko, O.A. & Avaeva, S.M. A malachite green procedure for orthophosphate determination and its use in alkaline phosphatase-based enzyme immunoassay. *Anal. Biochem.* **171**, 266–270 (1988).
31. Lazarus, M.B. *et al.* HCF-1 is cleaved in the active site of O-GlcNAc transferase. *Science* **342**, 1235–1239 (2013).
32. Schimpl, M. *et al.* *O*-GlcNAc transferase invokes nucleotide sugar pyrophosphate participation in catalysis. *Nat. Chem. Biol.* **8**, 969–974 (2012).
33. Martinez-Fleites, C. *et al.* Structure of an *O*-GlcNAc transferase homolog provides insight into intracellular glycosylation. *Nat. Struct. Mol. Biol.* **15**, 764–765 (2008).
34. Bai, M.Y. *et al.* Brassinosteroid, gibberellin, and phytochrome impinge on a common transcription module in *Arabidopsis*. *Nat. Cell Biol.* **14**, 810–817 (2012).
35. Oh, E. *et al.* Cell elongation is regulated through a central circuit of interacting transcription factors in the *Arabidopsis* hypocotyl. *eLife* **3**, e03031 (2014).
36. Gallego-Bartolomé, J. *et al.* Molecular mechanism for the interaction between gibberellin and brassinosteroid signaling pathways in *Arabidopsis*. *Proc. Natl. Acad. Sci. USA* **109**, 13446–13451 (2012).
37. Nozue, K. *et al.* Rhythmic growth explained by coincidence between internal and external cues. *Nature* **448**, 358–361 (2007).

38. Soy, J. *et al.* Phytochrome-imposed oscillations in PIF3 protein abundance regulate hypocotyl growth under diurnal light/dark conditions in *Arabidopsis*. *Plant J.* **71**, 390–401 (2012).
39. Silverstone, A.L., Mak, P.Y.A., Martínez, E.C. & Sun, T.P. The new *RGA* locus encodes a negative regulator of gibberellin response in *Arabidopsis thaliana*. *Genetics* **146**, 1087–1099 (1997).
40. Hart, G.W., Slawson, C., Ramirez-Correa, G. & Lagerlof, O. Cross talk between *O*-GlcNAcylation and phosphorylation: roles in signaling, transcription, and chronic disease. *Annu. Rev. Biochem.* **80**, 825–858 (2011).
41. Bond, M.R. & Hanover, J.A. A little sugar goes a long way: the cell biology of O-GlcNAc. *J. Cell Biol.* **208**, 869–880 (2015).
42. Greenboim-Wainberg, Y. *et al.* Cross talk between gibberellin and cytokinin: the *Arabidopsis* GA response inhibitor SPINDLY plays a positive role in cytokinin signaling. *Plant Cell* **17**, 92–102 (2005).
43. Tseng, T.S., Salomé, P.A., McClung, C.R. & Olszewski, N.E. SPINDLY and GIGANTEA interact and act in *Arabidopsis thaliana* pathways involved in light responses, flowering, and rhythms in cotyledon movements. *Plant Cell* **16**, 1550–1563 (2004).

Acknowledgments

We thank C. Toleman for assistance with *in vitro* enzyme assays and G. Dubay at Duke Chemistry Instrument Facilities for help with the MALDI–MS analysis. We also thank Z.-M. Pei and J. Siedow for helpful comments on the manuscript.

This work was supported by the National Institutes of Health (R01 GM100051 to T.-p.S.; R01 GM037537 to D.F.H.), the National Science Foundation (MCB-0923723 to T.-p.S.; MCB-0516690, MCB-0820666 and MCB-1158089 to N.E.O.), the Department of Energy (DE-SC0014077 to T.-p.S.) and the US Department of Agriculture (2014-67013-21548 to T.-p.S.).

Author contributions

R.Z., N.S. and T.-p.S. conceived and designed the research project. R.Z., N.S., W.-P.H. and J.H. performed molecular biology and biochemical analysis; R.Z., N.S., P.Z. and T.-p.S. analyzed data. B.B. performed LC–ETD–MS/MS analysis, and B.B., J.S. and D.F.H. analyzed MS data. P.Z. also provided advice on protein purification and structure modeling. M.B. provided reagents and advice for *in vitro* enzyme assays with MALDI–MS; N.E.O. provided experimental materials and shared unpublished results. R.Z., N.S. and T.-p.S. wrote the manuscript.

Competing financial interests

The authors declare no competing financial interests.

Additional information

Any supplementary information, chemical compound information and source data are available in the online version of the paper. Reprints and permissions information is available online at http://www.nature.com/reprints/index.html. Correspondence and requests for materials should be addressed to T.-p.S.

ONLINE METHODS

Plant materials, plant growth conditions and plant transformation. The *spy-8*, *spy-12*, *spy-15* and *spy-19* mutants were as previously described[15,39]. The DNA mutation (A to T at position 1994) in *spy-19* was identified by sequencing of PCR-amplified *spy-19* genomic DNA. For *in vitro* pulldown assays and MS analyses, a P_{RGA}:*FLAG-RGA* transgenic *Arabidopsis* line in the *sly1-10 rga-24* background[20] was crossed with *spy-8* to generate P_{RGA}:*FLAG-RGA sly1-10 spy-8 rga-24*. The F-box *sly1-10* mutation promotes accumulation of RGA[11].

Plant growth conditions were as previously described[44], with the following modifications: for affinity purification of FLAG-RGA protein for MS analysis, *Arabidopsis* seedling cultures were not supplemented with PuGNAc or glucosamine.

For the BR response, 2 μM propiconazole was included in the medium in addition to increasing concentrations of BL; for RT–qPCR analyses of DELLA, BZR1 and PIF target genes, seedlings were grown under constant light for 9 d. For tobacco agroinfiltrations, 3-week-old plants of *Nicotiana benthamiana* were used.

Statistical analyses. Statistical analyses were performed with the statistical package JMP Pro 10.0.2 (SAS Institute Inc.), with Student's *t* tests.

Plasmid construction. Primers for plasmid constructions are listed in **Supplementary Table 2**. All DNA constructs generated from PCR amplification were sequenced to ensure that no mutations were introduced.

For transient coexpression in tobacco, the 35S:His-FLAG-RGA^{GKG}, 35S:Myc-SPY and 35S:Myc-SEC constructs have previously been described[20]. To generate additional His-FLAG-AtDELLA constructs, the coding region of RGA in 35S:His-FLAG-RGA was substituted by the coding sequences of GAI, RGL1, RGL2 and RGL3 that had been cloned into pCR8/GW/TOPO[20]. For 35S:His-FLAG-GAI, 35S:His-FLAG-RGL1 and 35S:His-FLAG-RGL3 constructs, the 35S:His-FLAG-RGA construct was cut with BamHI and XbaI to remove the RGA sequence and was then ligated with DNA fragments of GAI (BamHI and XbaI), RGL1 (BamHI and XbaI) and RGL3 (BglII and SpeI), respectively. For 35S:His-FLAG-RGL2, 35S:His-FLAG-RGA was cut with BamHI and XmaI and ligated with the BglII–XmaI fragment from pCR8-RGL2 containing the RGL2 coding sequence. For constructs 35S:Myc-spy-8 and 35S:Myc-spy-12, cDNA from mutant plants was PCR-amplified with primers AtSPY-B1F and AtSPY-B2R, and the product was cloned into pDONR221 by BP recombination and moved into pEarlyGate-203 (ref. 45) through LR recombination. To generate 35S:Myc-spy-15, site-directed mutagenesis of pDONR221-SPY was performed with primers spy15+ and spy15− with the QuikChange Lightning strategy (Agilent Technologies). The resulting plasmid, pDONR221-spy-15, was then LR-recombined with pEarlyGate-203. To generate 35S:Myc-spy-19, the template pDONR221-SPY was PCR-amplified with primers attB1-site and spy-19-R, and attB2-site and spy-19-F. The two PCR products were mixed for a second round of amplification with primers attB1-site and attB2-site. The resulting product was cloned into pDONR207 by BP recombination and was moved in to pEarlyGate-203 by LR recombination. The 35S:3TPR-SPY construct was obtained by PCR amplification with primers 3TPR-SPY-ATG-F and SPY-STOP-R and cloning into pCR8/GW/TOPO (Thermo Fisher Scientific) and was moved to pEarlyGate-203 by LR recombination.

For *in vitro* enzyme assays, pTrc-His-MBP-3TPR-SPY and pTrc-His-MBP-5TPR-SEC constructs were generated by PCR amplification of 3TPR-SPY and 5TPR-SEC from pDONR221-SPY and pENTR1A-SEC, respectively, with primers SPY-TPR3/SPY- and SEC-TPR5/SEC-; the products were digested with BamHI and KpnI and cloned into the pTrc-His10-MBP-TEV vector derived from pTrcHisB (Thermo Fisher Scientific), a gift from J. Cho in the laboratory of P.Z. A similar procedure was used to create pTrc-His-MBP-3-TPR-spy-8, pTrc-His-MBP-3TPR-15 and pTrc-His-MBP-3TPR-19, except that the templates used were pDONR221-spy-8, pDONR221-spy-15 and pDONR207-spy-19, respectively. GST-fusion constructs for pulldown assays have previously been described[20,46].

Tobacco agroinfiltrations. Tobacco-leaf co-infiltration procedures were performed as previously described[20,47]. For most coexpression experiments, equal amounts of agrobacterium cultures with different expression constructs were mixed before infiltration. For the SPY and SEC competition experiments, cultures containing FLAG-RGA-GKG and Myc-SPY constructs were used at full strength (1×, OD_{600} of 0.6), whereas Myc-SEC was included at different dilutions (0.1×, OD_{600} of 0.06; 0.3×, OD_{600} of 0.2; 1×, OD_{600} of 0.6).

Protein purification for MS analysis. His-FLAG-RGA was purified from P_{RGA}:*FLAG-RGA* transgenic *Arabidopsis* lines in *rga-24 ga1-3* (WT for both *SPY* and *SEC*), *spy-8 rga-24 ga1-3* or *sec-3 rga-24 ga1-3* backgrounds. The tandem affinity purification procedures were as previously described[20], with the following modifications: 5 g of tissue from lines P_{RGA}:*FLAG-RGA sly1-10 rga-24* with or without *spy-8* or *sec-3* mutations was homogenized in three volumes (m/v) of buffer B. The cleared extract was incubated with 0.4 mL of His-Bind resin for 1.5 h at 4 °C and was loaded onto a disposable plastic column. The resin was washed with ten bed volumes of buffer B, then with ten bed volumes of buffer B supplemented with 20 mM imidazole, before elution. The second purification step was carried out with 5 μL of anti-FLAG-agarose beads (Sigma-Aldrich).

The purification procedure of His-FLAG-RGA^{GKG} from tobacco samples agroinfiltrated with 35S:His-FLAG-RGA^{GKG} alone or co-infiltrated with 35S:Myc-SPY or 35S:Myc-spy, 35S:Myc-3TPR-SPY or 35S:Myc-SEC was as described previously[20]. However, only 5 g of tissue per sample was used, and an additional wash with 20 mM imidazole in buffer B was included before elution from the His-Bind column.

Protein purification for *in vitro* enzyme assays. Recombinant 3TPR-SPY (spanning residues 326–914) was expressed in *E. coli* BL21 with an N-terminal His_{10}-MBP followed by a tobacco etch virus (TEV) protease–cleavage site (ENLYFQG/S). Cells were grown in LB medium at 37 °C until the absorbance at 600 nm (A_{600}) reached 0.5, at which point the culture was cooled on ice. The culture was then induced with 0.5 mM IPTG and incubated at 25 °C for 4 h. Cells were pelleted, resuspended in lysis buffer (50 mM NaH_2PO_4, pH 8.0, 300 mM NaCl, 10 mM imidazole and 10 mM 2-mercaptoethanol) and disrupted with a French pressure cell, then centrifuged at 40,000*g* for 60 min. The supernatant was incubated with Ni–NTA agarose Superflow resin (Qiagen), washed with ten column volumes of wash buffer (50 mM NaH_2PO_4, pH 8.0, 300 mM NaCl, 50 mM imidazole and 10 mM 2-mercaptoethanol), and eluted with four column volumes of elution buffer (50 mM NaH_2PO_4, pH 8.0, 300 mM NaCl, 250 mM imidazole and 10 mM 2-mercaptoethanol). The eluate was concentrated with centrifugal concentrators (Millipore) and buffer-exchanged into TEV digestion buffer (50 mM NaH_2PO_4, pH 7.5, 200 mM NaCl and 0.5 mM EDTA) before being treated with TEV protease at 4 °C for 16 h. A second Ni–NTA column was used to remove the His_{10}-MBP tag as well as the TEV protease. The target protein was further purified with size-exclusion chromatography (HiPrep Sephacryl S-300 HR, GE Healthcare). The final protein was concentrated to 10 mg/ml in storage buffer (20 mM Tris, pH 8.0, 50 mM NaCl and 1 mM DTT) and stored at −80 °C.

3TPR-spy mutants and 5TPR-SEC (spanning residues 356–977) were purified through a similar method, except that the His_{10}-MBP tag was not removed, to enhance the solubility of the purified protein.

Immunoblot analysis. To determine FLAG-RGA, Myc-SPY and Myc-SEC protein levels in *Arabidopsis* or tobacco tissues, total proteins were extracted and analyzed by SDS–PAGE and immunoblotting as previously described[48]. An anti-cMyc-HRP antibody (Sigma-Aldrich, cat. no. A5598; 8,000× dilution) was used to detect Myc-SPY. A monoclonal anti-FLAG-HRP antibody (Sigma-Aldrich, cat. no. A8592; 10,000× dilution) was used to detect FLAG-RGA. Anti-SEC antisera[20] (2,000× dilution) and anti-rabbit IgG-HRP (ThermoFisher, cat. no. 31462; 20,000× dilution) were used to detect Myc-SEC. Affinity-purified polyclonal anti-SPY antibodies (anti-LQKE[49]; 6,000× dilution), and anti-rabbit IgG-HRP (same as above) were used to detect recombinant WT and mutant SPY proteins for the *in vitro* enzyme assays and Myc-SPY in the tobacco samples. Validation for commercial antibodies is provided on the manufacturers' websites.

Identification of O-fucosylation and O-GlcNAc sites by LC–ETD and collisionally activated dissociation (CAD) MS/MS analyses. His-FLAG-RGA proteins

doi:10.1038/nchembio.2320

purified from *Arabidopsis* and tobacco were digested with trypsin and then separated by HPLC and analyzed by tandem MS with an Orbitrap Fusion Tribrid mass spectrometer equipped with ETD (Thermo Scientific)[50,51]. Sample processing and HPLC were as described previously[20]. MS^1 spectra were acquired in the Orbitrap at a resolution of 120,000, and this was followed by a data-dependent, 2-s Top-N MS/MS experiment alternating between CAD and ETD. Precursors were isolated with a resolving quadrupole with a 2-*m*/*z* window. MS^2 spectra were acquired in the linear ion trap at a normal scan rate, and ETD reaction times were varied according to the precursor charge state. Dynamic exclusion was turned on with a repeat count of 1 and exclusion duration of 10 s.

***In vitro* SPY and SEC activity assays by MALDI–MS.** Two RGA peptides were synthesized (ChinaPeptides) for the *in vitro* enzyme assays: peptide 1, FQGRLSNHGTSSSSSISK (amino acid residues 8–26, RGA^{pep1}); peptide 2, KSCSSPDSMVTSTSTGTQGGW (amino acid residues 166–183 +GGW, RGA^{pep2}). Each 20-µL reaction included 125 µM RGA peptide, 200 µM GDP–fucose (or UDP–GlcNAc, GDP–mannose, UDP–galactose and UDP–glucose in substrate-specificity test) and 10 µg 3TPR-SPY or 5TPR-SEC. For SPY, the reaction buffer contained 50 mM Tris-HCl, pH 8.2, 50 mM NaCl, 5 mM $MgCl_2$ (unless otherwise stated for buffer-condition optimization). For SEC, the reaction buffer contained 20 mM Tris-HCl, pH 7.2, and 12.5 mM $MgCl_2$. After incubation for 2 h (unless specified to be 16 h) at 25 °C, the peptides were purified with C18 Ziptips (MilliporeSigma) according to the manufacturer's protocol and analyzed by MALDI–MS with an Ultraflex II TOF/TOF mass spectrometer (Bruker Daltonics). Sample processing was performed as previously described[52]. For each reaction, 4 µL sample was mixed with 6 µL α-cyano-4-hydroxycinnamic acid (HCCA) matrix, and 1.2 µL of the mixture was spotted onto the plate and dried before being detected by MALDI–MS.

***In vitro* SPY activity assay with malachite green–coupled reactions.** *Kinetics.* Steady-state kinetics of 3TPR-SPY was determined through malachite green–coupled reactions, as previously described[29]. Briefly, a 130-µL reaction containing 50 mM Tris-HCl, pH 8.2, 50 mM NaCl, 5 mM $MgCl_2$, 50 µg of 3TPR-SPY, 0.5 µg of CD39L3 (NTPDase 3, R&D Systems) and different concentrations of substrates was incubated at 25 °C. 25-µL aliquots were collected at 2, 4, 6, 8 and 10 min and were separately inactivated at 95 °C for 30 s before free phosphate release was assayed with malachite green reagent. Kinetics parameters for GDP–fucose were measured with a fixed RGA^{pep1} concentration of 312.5 µM and varying GDP–fucose concentrations of 800, 400, 200, 100, 50, 25 and 12.5 µM. Kinetics parameters for the peptide were measured with a fixed GDP–fucose concentration of 800 µM and varying RGA^{pep1} concentrations of 100, 50, 37.5, 25, 12.5, 6.25, 3.125 and 1.56 µM. Data were fitted to Lineweaver–Burk plots to determine the kinetics parameters.

Activity assay of spy mutants. 25-µL reactions containing 50 mM Tris-HCl, pH 8.2, 50 mM NaCl, 5 mM $MgCl_2$, 125 µM RGA^{pep1}, 200 µM GDP–fucose, 0.1 µg of NPTDase-3 and 7 µg of 3TPR-SPY or mutant spy protein (His-MBP fusion proteins) were incubated for 10 min at 25 °C before being quenched and detected by malachite green reagent.

***In vitro* pulldown assays and RT–qPCR analysis.** Pulldown assays using *Arabidopsis* extracts and GST-fusion proteins produced in *E. coli* were carried out as previously described[20]. Recombinant GST, GST-BZR1, GST-PIF3 and GST-PIF4 bound to glutathione–Sepharose beads were used separately to pull down FLAG-RGA from protein extracts from P_{RGA}*:FLAG-RGA* transgenic *Arabidopsis* in *SPY sly1-10 rga-24* or *spy-8 sly1-10 rga-24* backgrounds.

For RT–qPCR analysis, total RNA was isolated from 9-d-old seedlings of *ga1-3*, *ga1-3 spy-8* and *ga1-3 spy-19* with a Quick-RNA MiniPrep kit (Zymo Reseaarch). First-strand cDNA was synthesized with a Transcriptor First Strand cDNA Synthesis kit (Roche Applied Science). For qPCR, FastStart Essential DNA Green Master Mix was used with a LightCycler 96 Instrument (Roche Applied Science).

***In silico* predictions of 3D protein structures.** SPY and SEC 3D structure models based on the human OGT structure (PDB 4N3C)[31] were generated with the online SWISS-MODEL Workspace (http://swissmodel.expasy.org/)[53,54]. 3D structure alignment, visualization and manipulations were performed with PyMOL (http://www.pymol.org).

Sequence alignment. Protein sequences were downloaded from the National Center for Biotechnology Information website, and sequence alignment was carried out with the DNAStar Lasergene Core Suite, version 12.0.0.

Data availability. All relevant data are included in the paper and in its Supplementary Text and Figures.

44. Zentella, R. *et al.* Global analysis of DELLA direct targets in early gibberellin signaling in *Arabidopsis*. *Plant Cell* **19**, 3037–3057 (2007).
45. Earley, K.W. *et al.* Gateway-compatible vectors for plant functional genomics and proteomics. *Plant J.* **45**, 616–629 (2006).
46. Dill, A., Thomas, S.G., Hu, J., Steber, C.M. & Sun, T.P. The *Arabidopsis* F-box protein SLEEPY1 targets gibberellin signaling repressors for gibberellin-induced degradation. *Plant Cell* **16**, 1392–1405 (2004).
47. Zhang, Z.L. *et al.* Scarecrow-like 3 promotes gibberellin signaling by antagonizing master growth repressor DELLA in *Arabidopsis*. *Proc. Natl. Acad. Sci. USA* **108**, 2160–2165 (2011).
48. Silverstone, A.L. *et al.* Repressing a repressor: gibberellin-induced rapid reduction of the RGA protein in *Arabidopsis*. *Plant Cell* **13**, 1555–1566 (2001).
49. Swain, S.M., Tseng, T.S., Thornton, T.M., Gopalraj, M. & Olszewski, N.E. SPINDLY is a nuclear-localized repressor of gibberellin signal transduction expressed throughout the plant. *Plant Physiol.* **129**, 605–615 (2002).
50. Udeshi, N.D., Compton, P.D., Shabanowitz, J., Hunt, D.F. & Rose, K.L. Methods for analyzing peptides and proteins on a chromatographic timescale by electron-transfer dissociation mass spectrometry. *Nat. Protoc.* **3**, 1709–1717 (2008).
51. Berk, J.M. *et al.* O-linked β-N-acetylglucosamine (O-GlcNAc) regulates emerin binding to barrier to autointegration factor (BAF) in a chromatin- and lamin B-enriched "niche". *J. Biol. Chem.* **288**, 30192–30209 (2013).
52. Xu, Y., Strickland, E.C. & Fitzgerald, M.C. Thermodynamic analysis of protein folding and stability using a tryptophan modification protocol. *Anal. Chem.* **86**, 7041–7048 (2014).
53. Arnold, K., Bordoli, L., Kopp, J. & Schwede, T. The SWISS-MODEL workspace: a web-based environment for protein structure homology modelling. *Bioinformatics* **22**, 195–201 (2006).
54. Biasini, M. *et al.* SWISS-MODEL: modelling protein tertiary and quaternary structure using evolutionary information. *Nucleic Acids Res.* **42**, W252–W258 (2014).